Scattering Profiles of Charged Gels: Frozen Inhomogeneities, Thermal Fluctuations, and Microphase Separation

Yitzhak Rabin* and Sergei Panyukov†

Department of Physics, Bar-Ilan University, Ramat-Gan 52900, Israel

Received June 6, 1996; Revised Manuscript Received September 25, 1996[⊗]

ABSTRACT: We calculate the scattering spectra of weakly charged, randomly cross-linked polymer gels in poor and in Θ solvents. For some values of the thermodynamic parameters, the competition between poor solubility, electrostatics, and network elasticity leads to the divergence of the structure factor at a wave vector q^*, signaling the onset of microphase separation in the gel. At the transition, the random inhomogeneous equilibrium monomer density profile of the gel is replaced by a periodically modulated density distribution. Unlike all other known cases of microphase separation, partial reorganization of the equilibrium state takes place even before the onset of the transition and leads to the appearance of a peak in the structure factor. Depending on the choice of thermodynamic parameters, the characteristic wavelength of the modulation varies from microscopic to macroscopic length scales. The ramifications of our results for neutron and light scattering experiments and for studies of phase transitions in polymer gels are discussed.

1. Introduction

Charged polymer gels are fascinating physical systems. Unlike neutral gels in which the volume varies continuously as one changes the quality of solvent, charged gels can undergo an abrupt volume transition upon change of temperature. Since charged gels are water soluble, their chemistry may be fine-tuned to reproduce much of the complexity of biological systems whose thermodynamics and kinetics results from a delicate interplay of electrostatics, hydrophobic interactions, hydrogen bonding, and van der Waals forces.[1] Due to their superabsorbing properties (some gels can swell by a factor of 1000!), they have numerous industrial applications.

In spite of their importance, our understanding of charged gels lags behind that of neutral ones. Part of the difficulty stems from the fact that attempts to construct a theory of gels must rely on input from the theory of polymer solutions, and while the theory of neutral polymer solutions is well-developed,[2,3] there is still considerable controversy in the area of polyelectrolyte solutions. Furthermore, the combination of long-range electrostatic interactions with the frozen inhomogeneous structure of gels leads to formidable mathematical difficulties in modeling these complex physical systems. Microscopic information about the structure of charged gels is limited because of the large number of experimentally tunable parameters such as the quality of solvent, concentration of preparation, degree of cross-linking, degree of ionization and of swelling, and concentration of added salt.

Recently, we developed a theory of neutral polymer gels which accounts for the frozen inhomogeneity of their structure as well as for the fact that gels behave as solids on large scales and as liquids on small scales (smaller than the length scale of monomer fluctuations in the network).[4−6] Since we now have a theory which is based on a solid formal ground and reproduces all the qualitative features observed in neutron and light scattering experiments on neutral gels (for a recent review of the experiments, see ref 7), we can attempt to apply our methods to charged gels. This program is carried out in the present work.

In section 2 we derive the electrostatic contribution to the free energy which governs the fluctuations of monomer concentration in a weakly charged network. The derivation is based on the random phase approximation, assuming that the fluctuations of the charge densities about their mean values are small, and results in a Debye−Hückel-type structure factor. We show that the monomer density correlation functions of charged gels can be obtained from their neutral counterparts simply by replacing the second virial coefficients in the state of preparation and in the final observed state by effective interaction coefficients which contain a wavelength-dependent electrostatic contribution due to screened Coulomb interactions. We present explicit analytic expressions for the total structure factor, for the correlator of static inhomogeneities, and for the correlator of thermal fluctuations in terms of the thermodynamic parameters in the state of preparation and in the final state of the gel. We analyze these expressions for the case of charged gels in Θ solvents and show that the scattering is suppressed by increasing the degree of ionization but is enhanced by the addition of salt. This effect has been observed in small-angle neutron scattering experiments.[8,9] The scattered intensity depends on the degree of ionization in the state of preparation, because the structure of network is affected by the degree of ionization of the polymer solution prior to cross-linking (electrostatic repulsions suppress density fluctuations in the pre-cross-linked polyelectrolyte solutions and result in more homogeneous networks). We compare the structure factors of charged gels at different degrees of cross-linking to that of a semidilute polyelectrolyte solution and show that the scattered intensity increases with the degree of cross-linking, the effect being most pronounced at $\mathbf{q} \rightarrow 0$, in agreement with experimental observations.[8,10] The form of the structure factor is determined by the interplay of two length scales: the characteristic length scale of static inhomogeneities which dominate the $\mathbf{q} \rightarrow 0$ scattering in neutral gels,[5] and an electrostatic length scale which produces a peak at a finite q in polyelectrolyte solutions.[11,12] For some values of the

† Permanent address: Theoretical Department, Lebedev Physics Institute, Russian Academy of Science, Moscow 117924, Russia.

[⊗] Abstract published in *Advance ACS Abstracts,* December 15, 1996.

S0024-9297(96)00826-1 CCC: $14.00

parameters, the presence of the two length scales leads to the appearance of a "shoulder" in the scattering profile.[13] We study the anisotropic scattering profiles of uniaxially stretched gels and show that, in Θ solvents, the $\mathbf{q} \rightarrow 0$ scattering is always enhanced in the direction of elongation and suppressed normal to it but that the effect is reversed at larger values of q. Enhancement of the scattering in the normal direction in the vicinity of $\mathbf{q}^*$ was reported in ref 9. We find that the magnitude of the scattered intensity is strongly enhanced and that the usual butterfly patterns (associated with enhanced scattering in the stretching direction) are recovered in the presence of salt, in agreement with experiment.[9]

In section 3 we study the instabilities associated with the divergence of the structure factor of a charged gel in a poor solvent. We distinguish between instabilities which take place at $\mathbf{q}^* \rightarrow 0$ (the spinodal for phase separation, SP) and which can be detected by light scattering and instabilities that occur at finite values of $\mathbf{q}^*$, typically within the range of wavelengths probed by neutron and X-ray scattering. The two instability lines in the (w,ϕ) plane (second virial coefficient vs monomer volume fraction) meet at the Lifshitz point,[14] at which the characteristic wavelength $1/q^*$ diverges. The instability lines and the Lifshitz point are affected by the presence of added salt and by uniaxial deformation. The wave vectors ($\mathbf{q}^*$) of the unstable modes are always oriented along the principal axes of compression.

Both the region of stability and the characteristic wave vector of the instability increase with the degree of cross-linking. In the absence of salt, the characteristic wavelength at the spinodal for microphase separation (MSP) lies in the range between the electrostatic length L_{BE} introduced by Borue and Erukhimovich[11] and the characteristic length scale of monomer fluctuations R which is of the order of the mesh size[4,5] (for physically reasonable choice of parameters, $L_{BE} \leq R$). As salt is added to the system, the stability region shrinks due to screening effects and the MSP approaches a limiting line which is independent of the degree of ionization.

The finite wavelength instability signals the onset of microphase separation, which is fundamentally different from weak crystallization in complex fluids such as polyelectrolyte solutions,[11,12] diblock copolymer melts,[15] and smectic liquid crystals.[16] In the latter systems, the appearance of a finite q peak in the structure factor as the transition point is approached reflects the enhancement of *thermal fluctuations* in the homogeneous liquid, on a length scale determined by the competition between the tendency to segregation and some physical mechanism which prevents phase separation on macroscopic length scales. In charged gels, the peak is dominated by scattering from static inhomogeneities and reflects the appearance of a *periodic modulation of the equilibrium density profile*. The modulation arises as the result of the interplay between the tendency to phase separation in a poor solvent which is opposed by the elastic forces in the network that suppress fluctuations on length scales larger than the monomer fluctuation radius and by long-range Coulomb interactions which suppress long-wavelength fluctuations of the counterion density. The existence of the peak in the correlator of static inhomogeneities implies that the density profile of the gel can be represented as a linear superposition of randomly oriented plane waves, with amplitudes peaked about $|\mathbf{q}| = q^*$. As the MSP is approached, these amplitudes grow and higher order nonlinear couplings become important. Although the investigation of the ordered mesophase is beyond the scope of this work, the interaction between the plane waves is expected to lead to the formation of lamellar domains, each of which is characterized by a director that lies along the axis defined by the local monomer density gradient. The directors of the domains can be ordered by the application of external forces such as mechanical deformations and electric fields (the latter couple to the spontaneous dipole moments of the domains).

We study the scattering profiles of charged gels in the vicinity of the microphase separation spinodal. In agreement with experimental results,[17] we find that the scattered intensity varies as q^{-4} away from the transition and that q^* deviates from a simple scaling behavior with concentration at the higher concentration range. The predicted exponent for the temperature dependence of the correlation length in the vicinity of the Lifshitz point ($\xi \sim |T - T_{LP}|^{-1/4}$) agrees with experimental observations.[25]

We examine the effect of uniaxial extension on the structure factors of charged gels. In the vicinity of $\mathbf{q}^*$, the scattering is always enhanced normal to the extension axis and suppressed along it and the total scattered intensity increases dramatically. The angular anisotropy of the structure factor in the $\mathbf{q} \rightarrow 0$ limit depends on the sign of the corresponding limit of the wave-vector-dependent effective interaction coefficient $\hat{w}_{\mathbf{q}}$ which contains a negative contribution of the second virial coefficient and a positive q-dependent electrostatic contribution. Thus, unlike the good or the Θ solvent case where the $\mathbf{q} \rightarrow 0$ scattering along the stretching axis is always larger than normal to it (this anisotropy gives rise to the butterfly effect[7]), in poor solvents the situation can be reversed near the spinodal, when the electrostatic contribution to $\hat{w}_{\mathbf{q}}$ is suppressed by the addition of salt or when the quality of solvent is reduced by changing the temperature.

In section 4 we summarize the main results of this work. The domain of applicability and the limitations of our theory are discussed. Finally, we comment on the comparison of the theory with experiments on polyelectrolyte gels and outline directions for future research.

2. Density Fluctuations and Static Inhomogeneities

Consider a charged gel prepared by instantaneous cross-linking of a solution of polyelectrolyte chains with average monomer concentration $\bar{\rho}^{(0)}$ and degree of ionization (fraction of charged monomers) $f^{(0)}$. The density of cross-links in the final state of the gel is $\nu = \bar{\rho}/(2\bar{N}) = \bar{\rho}R_c$, where $\bar{N}$ is the average number of chain monomers of size a between neighboring cross-links and R_c is the degree of cross-linking. The average monomer concentration and the ionization degree in the final state of the gel are $\bar{\rho}$ and f, respectively. We allow for the presence of monovalent salt of concentration $\bar{c}_s$ in the final state (i.e., the state in which the gel is studied) but assume, for simplicity, that the cross-linking was done in the absence of salt. In order to be as close as possible to the usual experimental conditions,[8,9] *we consider charged gels prepared in a good solvent and studied in a Θ or in a poor solvent.*

2.1. Free Energy Functional. We denote by ρ_i the counterion density due to both chain and salt counterions and by c_s the corresponding concentration of salt

co-ions and use Coulomb's law to relate the divergence of the local electric field $\mathbf{E}(\mathbf{x})$ to the local charge density,

$$\nabla\cdot\mathbf{E}(\mathbf{x}) = 4\pi e\epsilon[f\rho(\mathbf{x}) + c_s(\mathbf{x}) - \rho_i(\mathbf{x})] \quad (1)$$

Here, e is the unit electric charge and ϵ is the dielectric constant of the solvent. The electrostatic contribution to the free energy is given by

$$F_{ch}[\rho,\rho_i,c_s] = T\int d\mathbf{x}\left[\rho_i(\mathbf{x})\ln\frac{\rho_i(\mathbf{x})}{e} + c_s(\mathbf{x})\ln\frac{c_s(\mathbf{x})}{e} + \frac{\mathbf{E}^2(\mathbf{x})}{8\pi\epsilon}\right] \quad (2)$$

Assuming that the fluctuations of the various charge densities about their equilibrium values are small, one can derive the Debye−Hückel approximation to the screened electrostatic repulsion between the charged chains, which is valid for $\bar{c}_t\kappa^{-3} \gg 1$, where $\bar{c}_t = f\bar{\rho} + 2\bar{c}_s$ is the total density of small ions and κ^{-1} is the Debye screening length ($\kappa^2 \equiv 4\pi l_B\bar{c}_t$, where $l_B \equiv e^2/(\epsilon T)$ is the Bjerrum length). The electrostatic free energy functional of the monomer density,

$$F_{ch}[\rho] = -T\ln\int D\rho_i Dc_s \exp(-F_{ch}[\rho,\rho_i,c_s]/T) \quad (3)$$

can be easily evaluated in the random phase approximation by performing the Gaussian integrations over the small deviations $\delta\rho_i$ and δc_s of the corresponding charge densities from their mean values $\bar{\rho}_i$ and $\bar{c}_s$[18] (global electroneutrality imposes $\bar{\rho}_i = f\bar{\rho} + \bar{c}_s$). This yields the Debye−Hückel free energy

$$F^{DH}[\rho] = \frac{T}{2}\int\frac{d\mathbf{q}}{(2\pi)^3}\frac{|\rho_{\mathbf{q}}|^2}{s_{\mathbf{q}}^{DH}} \quad (4)$$

where

$$\frac{1}{s_{\mathbf{q}}^{DH}} = \frac{4\pi l_B f^2}{\kappa^2 + q^2} \quad (5)$$

is the inverse of the Debye−Hückel structure factor.

We proceed to calculate the total monomer density correlation functions which include both neutral chain and electrostatic contributions. Since we want to avoid difficulties associated with the non-Gaussian character of strongly charged chains,[19] we will consider only sufficiently small values of the degree of ionization f, for which one can neglect electrostatic effects on chain conformation. In order to make sure that the statistics of a segment of length $an(r)$ (r is the distance between the ends of the segment) is not strongly affected by electrostatic repulsion, we demand that the electrostatic energy is small compared to the thermal energy on this scale,

$$\frac{4\pi e^2 f^2 n^2(r)\exp(-\kappa r)}{\epsilon r} \le T \quad (6)$$

We distinguish between two cases. For $\kappa an^{1/2} < 1$, the left-hand side of eq 6 is an increasing function of r. Therefore, if condition (6) is satisfied on the length scale of a network chain, $f < \hat{l}_B^{-1/2}\bar{N}^{-3/4}$ ($\hat{l}_B \equiv 4\pi l_B/a$ is the dimensionless Bjerrum length), it will be automatically satisfied on smaller length scales. For $\kappa an^{1/2} > 1$ the above condition becomes $f < \hat{l}_B(\rho a^3)^3$ in the salt-free case and $f < \hat{l}_B^{1/4}(2\bar{c}_s a^3)^{3/4}$ at high concentrations of added salt (strong electrostatic screening). For the small degrees of ionization considered in this work,

$$f < \max\{\hat{l}_B^{-1/2}\bar{N}^{-3/4}, \hat{l}_B(\rho a^3)^3, \hat{l}_B^{1/4}(2\bar{c}_s a^3)^{3/4}\} \quad (7)$$

the electrostatic free energy, eq 4, can be added to the total free energy of a neutral gel given in ref 5 to which we will add a ρ^3 (third virial) term in order to stabilize the gel against collapse in a poor solvent in the absence of charges. The only effect of electrostatic interactions is to replace the second virial coefficients $w^{(0)}$ and w (w vanishes in a Θ solvent and is negative in a poor solvent) by effective virial coefficients. This has to be done for both the final state and the state of preparation:

$$w \to w_{\mathbf{q}} \equiv w + 1/s_{\mathbf{q}}^{DH}$$

and

$$w^{(0)} \to w_{\mathbf{q}}^{(0)} \equiv w^{(0)} + 1/s_{\mathbf{q}}^{(0)DH} \quad (8)$$

where $s_{\mathbf{q}}^{(0)DH}$ is obtained by substituting $\bar{c}_s = 0$, $f = f^{(0)}$ into eq 5 (we neglect the small difference between the Bjerrum lengths in the state of preparation and in the final state of the gel, which may differ due to the temperature dependence of this length). These effective virial coefficients will be used in all the expressions for the correlators.

2.2. Density Correlation Functions. 2.2.1. General Expressions for the Correlators. We begin with the general expressions for the monomer density correlation functions of a gel prepared in a good solvent and studied in a Θ or a poor solvent. Charged gels in good solvents will not be considered in this work since most of the qualitative features of their scattering profiles are expected to be quite similar to those of neutral gels.[20] In order to consider the effects of isotropic swelling and uniaxial extension on the magnitude and on the angular dependence of the scattered intensity, our general expressions will allow for both types of deformation.

Since thermal fluctuations of the monomer density are weak in the poor solvent regime, there is no renormalization of the parameters (virial coefficients, monomer size) in the final state of the gel.[4,5] Consequently, the *monomer fluctuation radius* is given by the Gaussian chain result, $R = a\bar{N}^{1/2}$, and the mean field expressions for the correlators can be applied throughout the entire q range. A slight complication arises in the short-wavelength limit since (as will be shown latter) the correlator of static inhomogeneities ($C_{\mathbf{q}}$) contains the structure factor in the state of preparation of the gel ($S_{\mathbf{q}}^{(0)}$) which, for $q \gg \xi^{-1}$ (ξ is the thermal correlation length), behaves as $q^{-4/3}$ instead of the mean field q^{-2} (recall that we assumed that the gel was prepared in a good solvent). We have shown, however, that the correlator of static inhomogeneities decays on length scales of the order of the monomer fluctuation radius R ($\gg\xi$),[5] and thus the use of the mean field instead of the scaling exponent in $S_{\mathbf{q}}^{(0)}$ has little effect on our results even in the limit $q \gg \xi^{-1}$.

The total structure factor of a charged gel in a Θ or a poor solvent is given by[5]

$$S_{\mathbf{q}} = G_{\mathbf{q}} + C_{\mathbf{q}} \quad (9)$$

where the contribution of thermal fluctuations is

$$G_{\mathbf{q}} = \frac{a^{-3}\phi\bar{N}\hat{g}_{\mathbf{q}}}{1 + \hat{w}_{\mathbf{q}}\hat{g}_{\mathbf{q}}} \tag{10}$$

and that of static density inhomogeneities is

$$C_{\mathbf{q}} = \frac{a^{-3}\phi\bar{N}}{(1 + \hat{w}_{\mathbf{q}}\hat{g}_{\mathbf{q}})^2(1 + Q^2)^2} \times \left[6 + \frac{9}{\hat{w}^{(0)}_{\lambda^*\mathbf{q}} - 1 + (Q_{\parallel}^2\lambda^2 + Q_{\perp}^2/\lambda)(\phi_{\mathrm{prep}}/\phi)^{2/3}\phi_{\mathrm{prep}}^{-1/4}/2}\right] \tag{11}$$

Here $Q \equiv a\bar{N}^{1/2}q$ is the dimensionless wave vector (we neglect the effect of electrostatics on the conformation of the chains) and $Q_{\parallel}$ and $Q_{\perp}$ are the projections of the wave vector along and normal to the stretching axis (the above expression includes the case of uniaxial deformation with stretching ratio λ). ϕ_{prep} and ϕ are the monomer volume fractions in the state of preparation and the final state, respectively. The function $\hat{g}_{\mathbf{q}}$ for gels in Θ and poor solvents was calculated in ref 5 (this function is the same for neutral and for charged gels) and is given by the expression

$$\hat{g}_{\mathbf{q}} \equiv \frac{g_{\mathbf{q}}}{\bar{\rho}\bar{N}} = \frac{1}{Q^2/2 + (4Q^2)^{-1} + 1} + \frac{2Q^2\phi^{2/3}\phi_{\mathrm{prep}}^{-5/12}}{(1 + Q^2)^2(Q_{\parallel}^2\lambda^2 + Q_{\perp}^2/\lambda)} \tag{12}$$

The quantity $\hat{w}^{(0)}_{\lambda^*\mathbf{q}}$ which appears in eq 11 is the dimensionless interaction parameter in the state of preparation, defined as

$$\hat{w}^{(0)}_{\lambda^*\mathbf{q}} \equiv w^{(0)}_{\lambda^*\mathbf{q}}\bar{\rho}^{(0)}\bar{N} = \phi_{\mathrm{prep}}^{5/4}\bar{N} + \frac{\hat{l}_{\mathrm{B}}(f^{(0)})^2\phi_{\mathrm{prep}}^{5/4}\bar{N}^2}{(Q_{\parallel}^2\lambda^2 + Q_{\perp}^2/\lambda)(\phi_{\mathrm{prep}}/\phi)^{2/3} + \hat{l}_{\mathrm{B}}f^{(0)}\phi_{\mathrm{prep}}^{5/4}\bar{N}} \tag{13}$$

where $\hat{l}_{\mathrm{B}} \equiv 4\pi l_{\mathrm{B}}/a$ is the dimensionless Bjerrum length. In deriving the above expression, it was assumed that no salt was present during the synthesis of the network.

The electrostatic modification of the second virial coefficient in the state of preparation changes the point at which the correlator of static inhomogeneities diverges (this divergence is associated with the divergence of the structure factor in the state of preparation of the network[5]). It was shown that, for neutral gels, this point is identical to the cross-link saturation threshold (CST) which defines the maximal degree of cross-linking, $R_{\mathrm{c}}^{\max} \equiv 1/(2\bar{N}^{\min}) \simeq (a^3\bar{\rho}^{(0)})^{5/4}$, that can be reached by instantaneous cross-linking of a polymer solution of monomer concentration $\bar{\rho}^{(0)}$.[4,5] The observation that gels can only be produced at concentrations higher than the overlap concentration c^* and are therefore topologically disordered solids[21] is valid for neutral as well as for charged gels (this follows from the geometrical origin of the above condition). However, in the latter case, the structure factor in the state of preparation does not diverge at c^* but rather at a lower concentration, $\bar{\rho}^{(0)} = a^{-3}[(1/\bar{N}) - f^{(0)}]^{4/5}$. Since the divergence of this structure factor leads to the appearance of frozen inhomogeneities of network structure on all the length scales in the gel, we conclude that the presence of charges in the state of preparation leads to the formation of more "homogeneous" networks. Consequently, the small-angle ($q \to 0$) scattered intensity from gels prepared from a charged polymer solution with degree of ionization $f^{(0)}$ should be smaller than from gels prepared from a neutral solution and subsequently charged to the same degree of ionization, $f = f^{(0)}$.

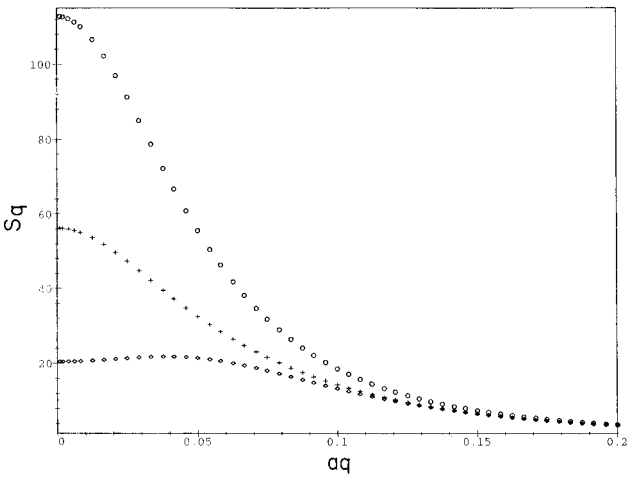

Figure 1. Dependence on the degree of ionization: the structure factor $S_{\mathbf{q}}$ of a gel studied at the concentration of preparation in a Θ solvent in the absence of salt is plotted as a function of the dimensionless wave vector aq. The monomer volume fraction in the state of preparation is $\phi_{\mathrm{prep}} = 0.05$ and the degree of cross-linking is $R_{\mathrm{c}} = 0.01$. The degrees of ionization at preparation and at the final state are $f^{(0)} = 0$, $f = 0.01$ (crosses), and $f^{(0)} = f = 0.01$ (diamonds). The case of a neutral gel $f^{(0)} = f = 0$ is shown for comparison (circles).

The dimensionless interaction parameter $\hat{w}_{\mathbf{q}}$ in eq 10 in the final state (a Θ or a poor solvent, depending on the value of w) is given by

$$\hat{w}_{\mathbf{q}} \equiv w_{\mathbf{q}}\bar{\rho}\bar{N} = \left(\frac{w}{a^3} + \phi\right)\phi\bar{N} + \frac{\hat{l}_{\mathrm{B}}f^2\phi\bar{N}^2}{Q^2 + \hat{l}_{\mathrm{B}}(f + 2\hat{c}_{\mathrm{s}})\phi\bar{N}} \tag{14}$$

The dimensionless salt concentration $\hat{c}_{\mathrm{s}} \equiv \bar{c}_{\mathrm{s}}/\bar{\rho}$ is defined as the ratio of the concentration of salt to the monomer concentration inside the gel. Note that the second virial coefficient w can be expressed in terms of the Flory interaction parameter χ as $w = a^3(1 - 2\chi)$ (in the poor solvent regime, $\chi > {}^1/_2$).

Since the general expressions for the density correlation functions contain many parameters, the investigation of the entire parameter space is impractical. In order to obtain some feeling about the scattering profiles, we first consider the case of charged gels in Θ solvents ($w = 0$) studied at the concentration of preparation, $\phi = \phi_{\mathrm{prep}}$.

2.2.2. Scattering Profiles in Θ Solvents. We consider a charged gel prepared in a good solvent and studied in the reaction bath (i.e., at the concentration of preparation) in a Θ solvent. In the following, the dimensionless Bjerrum length is taken to be $\hat{l}_{\mathrm{B}} = 10$.

In Figure 1 we study the dependence of $S_{\mathbf{q}}$ on the degree of ionization in the state of preparation ($f^{(0)}$) and in the final state of the gel (f). Note that in the case of a neutral gel ($f^{(0)} = f = 0$), the network is stabilized against collapse by the third virial coefficient, a^6. The small-q scattered intensity decreases monotonically with degree of ionization, in both the initial and the final state of the gel. The former effect is due to the modification of the effective interaction coefficient in the state of preparation, $\hat{w}^{(0)}_{\mathbf{q}}$, and was discussed in the previous subsection. Inspection of eqs 10 and 11 reveals that charges in the final state of the gel affect the

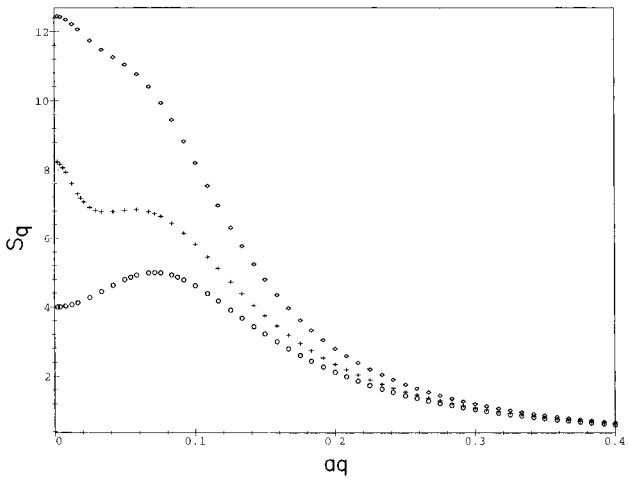

Figure 2. Dependence on the degree of cross-linking: plot of $S_{\mathbf{q}}$ vs aq for a gel studied at the concentration of preparation in a Θ solvent in the absence of salt. The monomer volume fraction in the state of preparation is $\phi_{prep} = 0.05$ and the degrees of ionization at preparation and at the final state are $f^{(0)} = f = 0.01$. The degree of cross-linking is $R_c = 0.005$ (diamonds) and 0.0017 (crosses). The structure factor of a polyelectrolyte solution of the same concentration and degree of ionization is shown for comparison (circles).

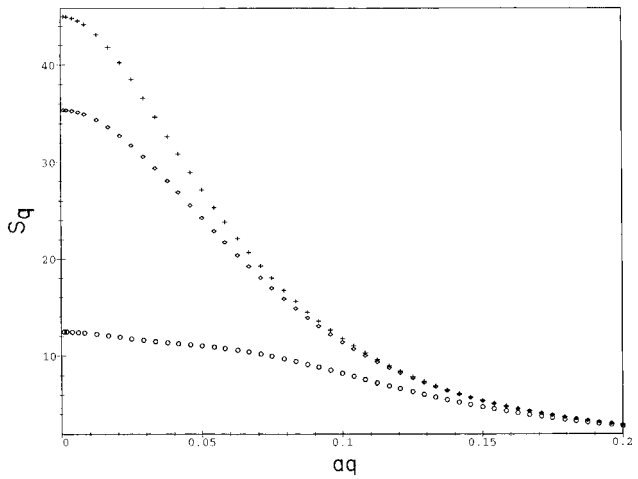

Figure 3. Dependence on concentration of salt: plot of $S_{\mathbf{q}}$ vs aq for a gel studied at $\phi = \phi_{prep} = 0.05$ in a Θ solvent. The degree of cross-linking is $R_c = 0.005$ and the electrostatic parameters are $f^{(0)} = f = 0.01$, $\hat{c}_s = 0$ (circles) and $f^{(0)} = f = 0.01$, $\hat{c}_s = 0.5$ (diamonds). The case of a neutral gel $f^{(0)} = f = 0$ is shown for comparison (crosses).

scattering profiles only through the presence of "screening"-type $(1 + \hat{w}_{\mathbf{q}}\hat{g}_{\mathbf{q}})$ factors in the denominators of the correlators of thermal fluctuations and of static inhomogeneities, which express the suppression of density variations by repulsive electrostatic interactions between the charged monomers and by the entropy of counterions. The screening of static density inhomogeneities is stronger than that of thermal fluctuations, because of the $(1 + \hat{w}_{\mathbf{q}}\hat{g}_{\mathbf{q}})^2$ factor in the denominator of eq 11, compared to the $(1 + \hat{w}_{\mathbf{q}}\hat{g}_{\mathbf{q}})$ factor in eq 10. While charge-induced suppression of thermal fluctuations is familiar from theories of polyelectrolyte solutions,[11,12] *the predicted effect of charges on the correlator of static inhomogeneities reflects the electrostatic modification of inhomogeneous equilibrium density profile of gels and has no counterpart in polyelectrolyte solutions.*

In Figure 2 we study the dependence of the structure factor on the degree of cross-linking R_c. The small-q scattered intensity increases monotonically with the degree of cross-linking, in agreement with experimental observations.[10] This effect is familiar from the theory of neutral gels,[4,5] and it originates from the fact that the intrinsic inhomogeneity of the network increases as the cross-link saturation threshold is approached at higher cross-link densities. The weak maximum at a finite q observed in the limiting case of a polyelectrolyte solution ($R_c = 0$) arises due to the competition between chain elasticity and electrostatics.[11,12] The above maximum is present in weakly cross-linked gels but turns into a "shoulder" and eventually disappears as the degree of cross-linking is increased (see Figure 1). This phenomenon has been observed in experiments.[10,13] Although a peak at a finite q appears at both polyelectrolyte solutions and gels, its origin is quite different in the two cases: *while in the former the maximum is associated with thermal fluctuations about the homogeneous concentration profile of a liquid, in the latter it appears in the correlator of static inhomogeneities of a solid and we conclude that the equilibrium density profile of the gel becomes periodically modulated.* This point will be discussed in greater detail in the next section where we consider microphase separation in poor solvents.

The effect of added salt on the scattering profiles of charged gels studied at the concentration of preparation in Θ solvents is shown in Figure 3. As expected, the addition of salt screens the electrostatics and increases the scattered intensity at small q.[9] Although at the high salt concentration shown ($\hat{c}_s = 0.5$), all electrostatic effects in the final state of the gel are nearly completely screened, the small-q limit of the total structure factor is still considerably smaller than that of the neutral gel. This surprising observation is the consequence of the "frozen-in" network structure which is fixed once and for all during the formation of the gel. Information about this structure is contained in the correlator of static inhomogeneities $C_{\mathbf{q}}$ which "remembers" that the network was formed by cross-linking a polyelectrolyte solution in the absence of added salt (recall that we assumed $f^{(0)} = 0.01$ and $\hat{c}_s^{(0)} = 0$) and, therefore, the intrinsic heterogeneity of network structure is smaller than for a gel prepared from a neutral polymer solution.

We turn to examine the effect of uniaxial extension on the scattering profiles and compare the structure factors at wave vectors parallel and perpendicular to the stretching direction for weakly ($f^{(0)} = 0.01$, $f = 0.03$) and strongly charged ($f^{(0)} = 0.01$, $f = 0.1$) gels. Although the higher degree of ionization ($f = 0.1$) falls outside the range of validity of our theory, our qualitative results should apply even in this regime since corrections to the free energy due to deviations from Gaussian statistics of strongly charged chains are expected to be small compared to the counterion entropy which is taken into account exactly in our approach. In Figure 4 we observe that the scattered intensity at $q \to 0$ is always larger along the stretching axis than normal to it and that the situation is reversed in the limit of large q. Note that while $S_{\mathbf{q}\parallel}$ is a monotonically decreasing function of the wave vector, $S_{\mathbf{q}\perp}$ has a maximum at a finite value of q. We will show later that this maximum is a characteristic signature of the strain-induced rearrangement of the inhomogeneous monomer density profile into a periodic pattern normal to the stretching axis. The small-q angular anisotropy, $S_{\mathbf{q}\parallel} - S_{\mathbf{q}\perp}$, results in the appearance of butterfly patterns in contour plots of the scattered intensity. Since the anisotropy decreases with increasing degree of ionization, we expect butterfly patterns in small-angle neutron scattering from weakly

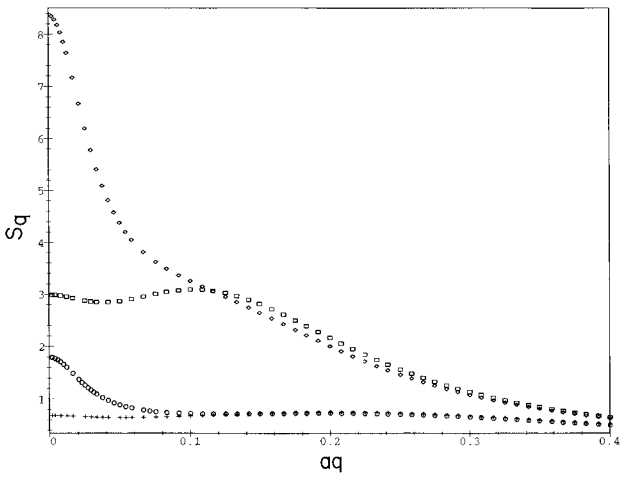

Figure 4. Effect of uniaxial extension ($\lambda_{||} = 1.4$) on gels studied at $\phi = \phi_{prep} = 0.05$ in a Θ solvent in the absence of salt. The degree of cross-linking is $R_c = 0.005$. For degrees of ionization $f^{(0)} = 0.01$, $f = 0.03$, the structure factors for wave vectors along ($S_{q||}$) and normal ($S_{q\perp}$) to the stretching axis are shown by diamonds and squares, respectively. For $f^{(0)} = 0.01$, $f = 0.1$, the corresponding structure factors are given by circles and crosses.

charged gels. In strongly charged gels, this angular anisotropy may be too weak to be detected in the neutron scattering range (experiments report that the butterfly pattern disappears at high degrees of ionization[9]) but, since the anisotropy increases with the wavelength, it could be observed by light scattering.

3. Microphase Separation

3.1. General Considerations. Inspection of our expressions for the density correlation functions shows that, for some choices of parameters, the amplitude of density variations in the gel diverges. Since dramatic enhancement of scattering is usually associated with the proximity of a spinodal line at which long-wavelength fluctuations diverge, it is important to understand the nature of the associated phase transition. Analysis of the phase diagrams shows that, under conditions of equilibrium swelling in excess solvent, the gel becomes unstable against a volume transition into a new homogeneous state of different monomer concentration, before the spinodal for phase separation is reached.[22,23] This is related to the observation that while the osmotic bulk modulus K vanishes at the spinodal of the volume transition, the longitudinal modulus $E_L = K + 4\mu/3$ vanishes at the spinodal for phase separation.[24] Since the shear modulus μ is always positive, we conclude that the latter spinodal can be reached only upon further decrease of the quality of solvent.

Physically, the difference between the two spinodals stems from the fact that while the appearance of concentration inhomogeneities is always accompanied by increased elastic stresses in the network, the latter are actually reduced during the homogeneous deswelling of the gel. The spinodal of the volume transition corresponds to the stability limit of the gel with respect to a uniform change of its volume and therefore is not related to the divergence of the structure factor which signals the appearance of an instability with respect to phase separation into regions of different monomer concentrations. Although the point at which $S_{\mathbf{q}\to 0}$ diverges cannot be reached under equilibrium swelling conditions, it can be observed experimentally if the volume transition is suppressed by fixing the surface of the gel or by removing it from the solvent bath.

In the following we will consider gels in which the volume transition is prevented by some external means and which are maintained at a fixed monomer volume fraction ϕ. We will refer to the spinodal of phase separation where $S_{\mathbf{q}}$ diverges as the "spinodal" and will distinguish between spinodals for phase separation (SP) and for microphase separation (MSP), depending on whether the divergence takes place at $\mathbf{q} = 0$ or at a finite $\mathbf{q}$. The SP of gels is the analog of the usual spinodal of phase separation in binary liquids and contains a critical point at which two coexisting phases merge (i.e., have identical concentrations).

The divergence of the long-wavelength structure factor has a simple experimental consequence: at this point, the amplitude of the long-wavelength density variations becomes very large and, as the result of strong scattering of light off these fluctuations, the transparent gel becomes opaque. If we vary any two of the thermodynamic parameters while keeping the others fixed, the set of points at which $S_{\mathbf{q}\to 0}$ diverges generates a line in the plane spanned by these two parameters. Inspection of eqs 10 and 11 shows that the SP obeys the equation

$$1 + \hat{w}_{\mathbf{q}}\hat{g}_{\mathbf{q}}|_{q=0} = 0 \qquad (15)$$

which defines a relation between any two thermodynamic parameters of the gel. Using eqs 12 and 14 for a swollen but unstretched ($\lambda = 1$) gel, this equation becomes

$$\frac{w}{a^3} + \frac{\phi_{prep}^{5/12}}{2\bar{N}\phi^{5/3}} + \phi + \frac{f^2}{\phi(f + 2\hat{c}_s)}\Big|_{SP} = 0 \qquad (16)$$

In the limit of large excess of added salt ($\hat{c}_s \gg f$), this expression reduces to the SP of an uncharged ($f = 0$) gel in a poor solvent, as electrostatic repulsions are strongly screened.

Let us consider the possibility that the density correlation function diverges at some finite wave vector $\mathbf{q}^*$. In liquids, this divergence is usually interpreted as the onset of instability of the homogeneous phase with respect to the formation of a spatially modulated phase (*microphase separation* transition). Under good solvent conditions, gels are characterized by a random inhomogeneous density profile and the correlation length associated with these static inhomogeneities is of the order of the monomer fluctuation radius R.[4,5] The microphase separation transition in charged gels in poor solvents corresponds to the appearance of a spatially modulated density profile, with period $2\pi/q^*$. Since, as will be shown later, under most conditions this characteristic wavelength is $\leq R$, we conclude that *microphase separation in polymer gels is a transition from a disordered to an ordered microstate of the network, at which the random equilibrium density distribution is replaced by a regular periodic density profile.*

We proceed to derive the spinodals for arbitrarily swollen and uniaxially deformed gels. The MSP is defined by the conditions that both the function $1 + \hat{w}_{\mathbf{q}}\hat{g}_{\mathbf{q}}$ and its derivative with respect to the wave vector vanish at $q = q^*$ (the two conditions define the MSP line and the characteristic wave vector q^*). Since the spinodal depends on the direction of the deformation, when the quality of solvent is reduced, the instability takes place for wave vectors along the direction for which the condition $1 + \hat{w}_{\mathbf{q}}\hat{g}_{\mathbf{q}} = 0$ is satisfied for the first time. Inserting the expressions for $\hat{g}_{\mathbf{q}}$ and $\hat{w}_{\mathbf{q}}$ into

the above conditions, one obtains the following equations for the characteristic wave vector q^* and for the MSP of a uniaxially deformed and swollen gel,

$$\frac{w}{a^3} + \Gamma(Q^2)|_{Q^*=Rq^*} = 0, \qquad \left.\frac{d\Gamma(Q^2)}{d(Q^2)}\right|_{Q^*=Rq^*} = 0 \quad (17)$$

where the function $\Gamma(Q^2)$ is defined by

$$\Gamma(Q^2) \equiv \phi + \frac{1}{\bar{N}\phi}\left[\frac{1}{1 + Q^2/2 + 1/(4Q^2)} + \frac{2\phi^{2/3}\phi_{prep}^{-5/12}}{h(\lambda)(1+Q^2)^2}\right]^{-1} + \frac{f^2}{\phi(f + 2\hat{c}_s) + Q^2/(\hat{l}_B\bar{N})} \quad (18)$$

Inspection of eq 12 shows that one should substitute $h(\lambda) = \lambda^2$ when $\lambda < 1$ and $h(\lambda) = \lambda^{-1}$ when $\lambda > 1$. The instability first appears for fluctuation modes with wave vector **q*** directed along the principal axes of compression. Thus, under uniaxial compression or biaxial extension ($\lambda < 1$), **q*** points along the compression axis. Under uniaxial extension or biaxial compression ($\lambda > 1$) **q*** lies in the plane normal to the axis of elongation.

Inspection of eqs 17 and 18 shows that, in the limit of small concentrations, the MSP becomes universal and occurs always at $q^* = (2^{1/4}a\bar{N}^{1/2})^{-1}$, and we conclude that for $\phi \to 0$ the critical wavelength at the MSP is of the order of the average chain size. In this limit electrostatic effects are negligible and microphase separation occurs as the result of the interplay between poor solvent and elastic effects.

We can rewrite the SP condition, eq 15, in terms of the function $\Gamma(Q^2)$

$$\frac{w}{a^3} + \Gamma(0)\Big|_{SP} = 0 \quad (19)$$

For uniaxially deformed gels this condition is satisfied at smaller values of $|w|$ than predicted for unstretched gels (eq 16), and we conclude that *uniaxial deformations always destabilize the gel against concentration variations along the principal axes of compression*.

For some combinations of thermodynamic parameters one may reach the so-called *Lifshitz point* (LP) at which the MSP occurs at $q^* \to 0$.[14] Using eqs 17 and 18, we can represent the conditions that define this point in the form

$$\frac{w}{a^3} + \Gamma(0)\Big|_{LP} = 0, \quad \left.\frac{d\Gamma(Q^2)}{dQ^2}\right|_{Q=0} = 0, \quad \left.\frac{d^2\Gamma(Q^2)}{(dQ^2)^2}\right|_{Q=0} > 0 \quad (20)$$

The first of these equations coincides with the definition of the SP, eq 16, and it can be shown that the third inequality in eq 20 is satisfied for any choice of the parameters. The second equation can be rewritten as

$$\frac{f}{f + 2\hat{c}_s} - \left[\hat{l}_B h(\lambda)\phi_{prep}^{5/12}\left(\phi^{1/3} - \frac{h(\lambda)\phi_{prep}^{5/12}}{\phi^{1/3}}\right)\right]^{1/2}\Big|_{LP} = 0 \quad (21)$$

Inspection of this equation shows that, depending on the degree of ionization and on the concentration of added salt, the LP exists only in the range of concentrations defined by

$$\phi_{LP}^{s} \le \phi_{LP} \le \phi_{LP}^{ns} \quad (22)$$

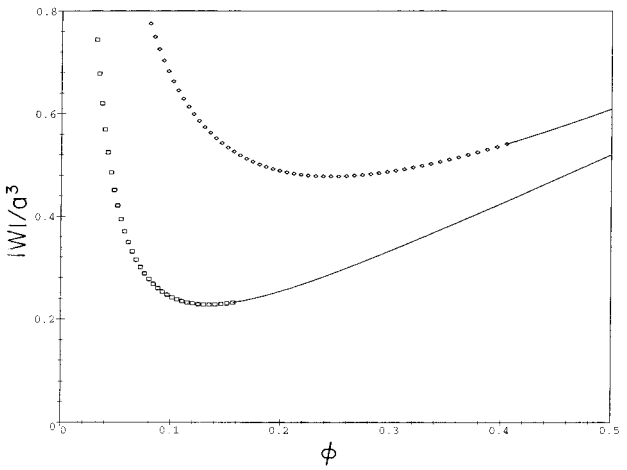

Figure 5. MSP in the $|w|a^{-3}$ vs ϕ plane for undeformed gels ($\lambda = 1$). The parameters of preparation are $\phi_{prep} = 0.05$, $R_c = 0.01$, and $f^{(0)} = 0$, and the degree of ionization is $f = 0.05$. The MSP's are shown by diamonds and by boxes for the no added salt and the excess salt ($\hat{c}_s = 0.1$) cases, respectively. The SP's are shown by solid lines and meet the MSP's at the corresponding Lifshitz points.

where the lower bound,

$$\phi_{LP}^{s} \equiv [h(\lambda)]^{3/2}\phi_{prep}^{5/8} \quad (23)$$

corresponds to the limit of large salt concentration. The upper bound,

$$\phi_{LP}^{ns} = [h(\lambda)]^{3/2}\phi_{prep}^{5/8}\left[\left(1 + \frac{1}{4\hat{l}_B^2[h(\lambda)]^3\phi_{prep}^{5/4}}\right)^{1/2} + \frac{1}{2\hat{l}_B[h(\lambda)]^{3/2}\phi_{prep}^{5/8}}\right]^3 \quad (24)$$

corresponds to the no added salt case. In both cases the volume fraction at the LP is independent of the degree of ionization f. The volume fraction ϕ_{LP} is always larger than ϕ_{prep} for unstretched gels but can be either larger or smaller than ϕ_{prep} for gels subjected to uniaxial extension. Analysis of eq 24 shows that in the absence of salt, the volume fraction at the LP is always larger than $(\phi_{LP}^{ns})^{min} = 4/\hat{l}_B \approx 0.4$. We conclude that in this case the Lifshitz point can be reached only at very high concentrations and that under most circumstances only microphase separation will be observed.

Note that in the limit $\hat{c}_s \to \infty$, the concentration at the Lifshitz point, $\phi_{LP} = \phi_{prep}^{5/8}$, coincides with that of a neutral gel ($f = 0$). The difference between this value and our previous mean-field result for neutral gels,[4] $\phi_{LP} \simeq \phi_{prep}$, stems from our present assumption that the gel was prepared in a good solvent.

The existence of a Lifshitz point has profound ramifications for scattering studies of phase separation in charged gels. When microphase separation takes place away from this point, the wavelength of the microstructure is, in general, outside the light scattering regime and can only be observed by neutron or X-ray scattering. When the LP is approached, the wavelength at which the scattered intensity diverges moves to the visible range and the gel becomes opaque.

In Figure 5 we plot the instability lines in the (w,ϕ) plane for charged unstretched gels, both in the absence and in the presence of salt. The MSP and the corresponding SP meet at the Lifshitz point. In the absence of salt this point lies in the concentrated regime

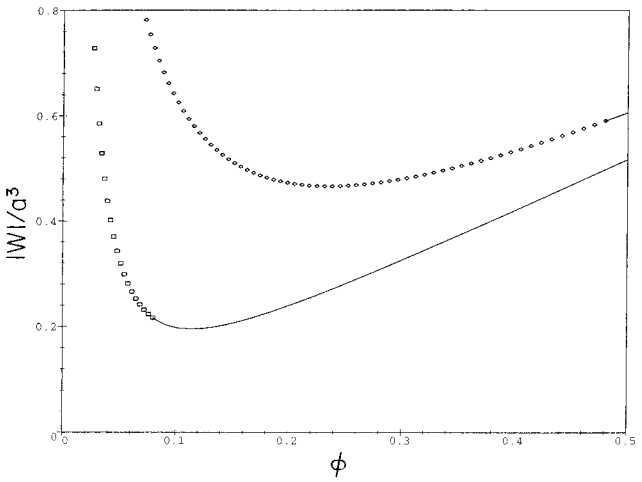

Figure 6. MSP in the $|w|a^{-3}$ vs ϕ plane for uniaxially compressed gels ($\lambda = 0.8$). All other parameters and notations are the same as in Figure 5.

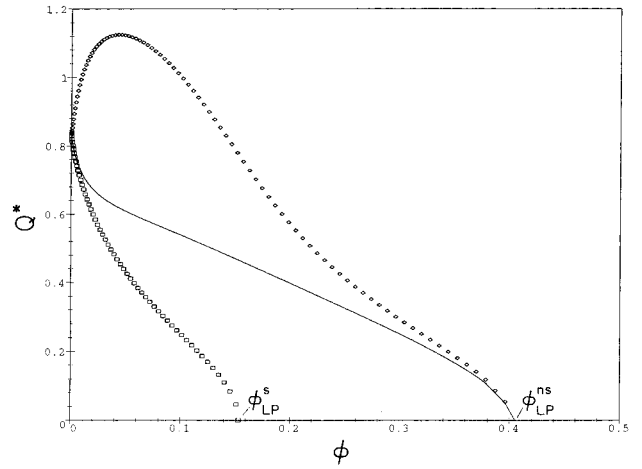

Figure 7. Variation of the critical wave vector q^* with concentration ϕ for undeformed gels. The parameters of preparation are the same as in Figure 5. The curves for $f = 0.05$, $\hat{c}_s = 0$; $f = 0.01$, $\hat{c}_s = 0$; and $f = 0.01$, $\hat{c}_s = 1$ are shown by diamonds, solid line, and boxes, respectively. The volume fractions at the Lifshitz points in the absence (ϕ^{ns}_{LP}) and in the presence of salt (ϕ^{s}_{LP}) are indicated.

($\phi \approx 0.4$) where the high concentration of charges produces strong screening and allows long-wavelength density modulations. The addition of salt destabilizes the gel against long-wavelength concentration variations and shifts the LP to lower concentrations, thus decreasing the range over which microphase separation at a finite q^* takes place. In Figure 6 we study the effect of uniaxial compression (or biaxial extension) on the instability lines, for critical wave vectors **q*** which point along the principal axes of compression. The deformation destabilizes the gel and increases the range over which microphase separation at a finite q^* takes place in the absence of added salt. In the presence of salt, the destabilization effect is somewhat stronger and the LP moves to smaller concentrations.

In Figure 7 we plot the critical wave vector q^* at the MSP vs the monomer volume fraction ϕ. For weakly ionized gels in the absence of salt and for gels studied in the presence of excess salt, q^* decreases monotonically with increasing concentration until the corresponding LP's are reached. At higher degrees of ionization (in the absence of salt), the behavior is non-

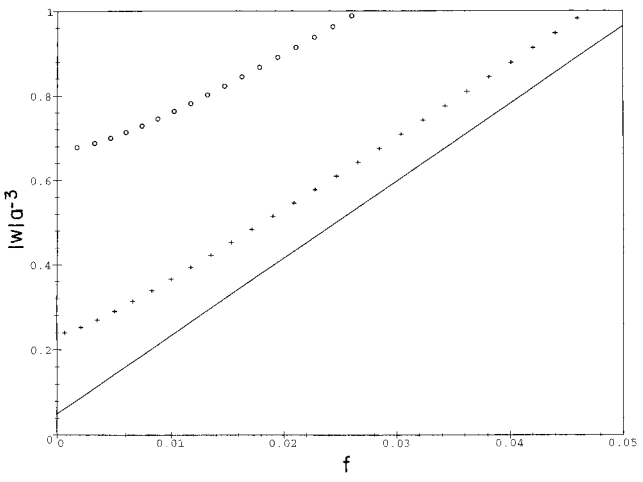

Figure 8. MSP in the $|w|a^{-3}$ vs f plane for gels studied at $\phi = \phi_{prep} = 0.05$ in a poor solvent in the absence of salt. The degrees of cross-linking are $R_c = 0.017$ (circles) and 0.005 (crosses). The MSP for a polyelectrolyte solution is shown by the solid line.

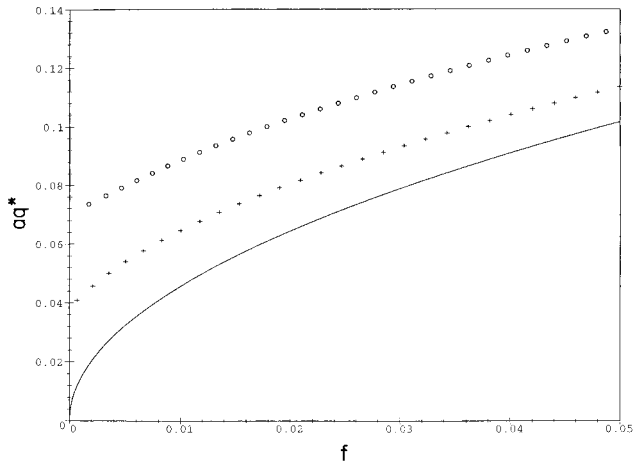

Figure 9. Critical wave vector aq^* at the MSP is plotted vs the degree of ionization. The parameters are the same as in Figure 8.

monotonic and q^* first increases and then decreases with ϕ. The initial increase corresponds to the Borue–Erukhimovich[11] regime where electrostatic effects dominate. At higher monomer (and counterion) concentrations, electrostatic screening becomes strong and the subsequent decrease of q^* with ϕ is dominated by the reduction of elastic restoring forces as the concentration is increased. Both the universal behavior at $\phi \to 0$ and the fact that in the absence of salt the LP does not depend on the degree of ionization are clearly observed in Figure 7.

3.2. Scattering Profiles in the Vicinity of the MSP. We now turn to the analysis of scattering profiles of charged gels in poor solvents. In Figure 8 we present the MSP line in the ($|w|/a^3$,f) plane and show how it varies with the degree of cross-linking for gels studied at the concentration of preparation in the absence of added salt. The line corresponding to polyelectrolyte solutions[11] ($|w| \propto f$) is shown for comparison. Note that the stable region lies below the MSP and increases with the degree of cross-linking. The stabilizing effect of cross-links follows from the observation (see Figure 9) that for $\phi = \phi_{prep}$, the characteristic wavelength ($2\pi/q^*$) at the microphase separation transition decreases with increasing degree of cross-linking and is always smaller

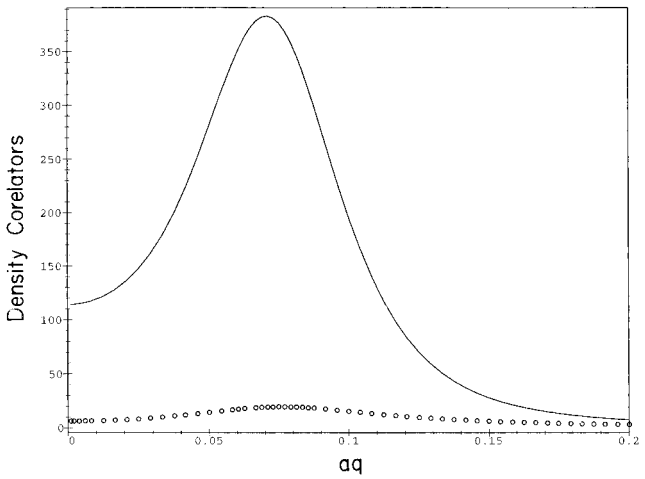

Figure 10. Structure factor $S_{\mathbf{q}}$ (line) and the thermal correlator $G_{\mathbf{q}}$ (circles) for gels studied at $\phi = \phi_{prep} = 0.05$ in a poor solvent ($|w|a^{-3} = 0.3$) in the absence of salt. The parameters are $R_c = 0.005$ and $f^{(0)} = 0$, $f = 0.01$.

than the Borue−Erukhimovich length[11,12]

$$L_{BE} \simeq \frac{a}{f^{1/2}(\hat{l}_B \phi_{prep})^{1/4}} \tag{25}$$

Since the energy penalty for concentration variations increases with the wave vector, the upward shift of the wave vector q^* stabilizes the gel against microphase separation. For fixed degree of cross-linking, q^* decreases with decreasing degree of ionization and is finally pinned down at a value proportional to the inverse monomer fluctuation radius $R^{-1} = (a\tilde{N}^{1/2})^{-1}$ which determines the length scale of static inhomogeneities in the network. Although there are no direct experimental observations of microphase separation in charged gels, a qualitative comparison can be made with studies in which a peak at finite q was reported. In agreement with our results, it was found that the position of the peak shifts to higher q values and that its amplitude decreases as one increases the degree of ionization.[8]

Inspection of our expressions for the correlators, eqs 10 and 11, shows that as the MSP is approached, the main contribution to the total structure factor comes from the correlator of static inhomogeneities (see Figure 10). As $w \to w_{MSP}$ and $\mathbf{q} \to \mathbf{q}^*$, the structure factor diverges as

$$S_{\mathbf{q}\to\mathbf{q}^*} \sim \frac{1}{[w - w_{MSP} + c(\mathbf{q}^2 - \mathbf{q}^{*2})^2]^2} \tag{26}$$

where w_{MSP} is the second virial coefficient at the MSP and c is some function of the MSP parameters which does not depend on w or on $\mathbf{q}$. For $\mathbf{q}^{*2} > 0$ the amplitude of the peak diverges as $(w - w_{MSP})^{-2}$ and its width vanishes as $(w - w_{MSP})^{1/2}$. Away from the LP the correlation length at the MSP diverges as

$$\xi_{MSP} \propto (q^*)^{-1}(w - w_{MSP})^{-1/2} \sim |T - T_{MSP}|^{-1/2} \tag{27}$$

where T_{MSP} is the temperature at the MSP. At the LP the correlation length diverges as

$$\xi_{LP} \sim |T - T_{LP}|^{-1/4} \tag{28}$$

where T_{LP} is the Lifshitz point temperature. A $^1/_4$ exponent was indeed observed in flow measurements of the friction coefficient ($\propto\xi$) on neutral NIPA gels studied at the concentration of preparation[25] (recall that in neutral gels prepared in Θ solvents, the LP is reached at this concentration[4]). Some care must be exercised in relating the above observation to our results since the presence of hydrogen bonding in NIPA gels may lead to the breakdown of the Flory-type virial expansion of the free energy[26] used in the present work.

The observation that the structure factor diverges at the MSP implies that the gel reorganizes itself into a periodically modulated structure, with a characteristic wavelength $2\pi/q^*$. Although analogous microphase separation transitions take place in complex liquid systems such as melts of diblock copolymers, polyelectrolyte solutions, and smectic mesophases of liquid crystals, the onset of weak crystallization in these systems is signaled by the growth of amplitude of thermal density fluctuations at a wave vector $\mathbf{q}^*$, as the transition point is approached. The above systems remain homogeneous liquids up to the transition point and the ordered mesophase appears only beyond the MSP. In charged gels in the vicinity of the MSP, both $G_{\mathbf{q}} \propto (1 + \hat{w}_{\mathbf{q}}\hat{g}_{\mathbf{q}})^{-1}$ and $C_{\mathbf{q}} \propto (1 + \hat{w}_{\mathbf{q}}\hat{g}_{\mathbf{q}})^{-2}$ have a maximum at $\mathbf{q}^*$, but $C_{\mathbf{q}^*} \gg G_{\mathbf{q}^*}$ (see Figure 10). Since $C_{\mathbf{q}}$ describes the variations of the equilibrium density profile of the network, we conclude that as the MSP is approached, the random inhomogeneous density distribution is reorganized into a new equilibrium profile which can be described as a linear combination of plane waves, the amplitudes of which are peaked about $|\mathbf{q}| = q^*$. These amplitudes grow with further approach to the MSP and plane waves corresponding to different directions of $\mathbf{q}$ begin to interact. Such interactions are described by higher order terms in the deviations from the mean density and lead to the appearance of lamellar domains, each of which is characterized by a different direction of the wave vector $\mathbf{q}$. Strictly speaking, the consideration of these nonlinear effects is beyond the domain of applicability of the RPA approximation used in this work and therefore we can not prove that a lamellar structure will result, although its plausibility is supported by symmetry arguments (the symmetry between high- and low-density regions in the gel is analogous to the situation in symmetric diblocks). In view of the above, we conjecture that the MSP corresponds to an orientational ordering transition, i.e., to the appearance of domains characterized by local uniaxial ordering of the gradients of monomer concentration in the gel.

We turn to study the scattering profiles of gels subjected to uniaxial extension under conditions close to the MSP. In Figure 11 we present the structure factors $S_{\mathbf{q}\|}$ and $S_{\mathbf{q}\perp}$, with wave vectors parallel and perpendicular to the stretching axis, respectively, for gels studied at the concentration of preparation in the absence of salt. The $\mathbf{q} \to 0$ scattered intensity is slightly enhanced along the stretching axis and suppressed normal to it. In the vicinity of the peak ($\mathbf{q}^*$), there is dramatic enhancement of the scattering in the direction normal to the stretching axis while the intensity along this axis decreases monotonically with $\mathbf{q}$ and falls below the unstretched gel value. Since the thermal contribution to the scattering is negligible, we conclude that uniaxial extension modifies the equilibrium structure of the gel by orienting the monomer concentration gradients along the principal axes of compression (uniaxial orientation of the concentration gradients can be produced by biaxial extension).

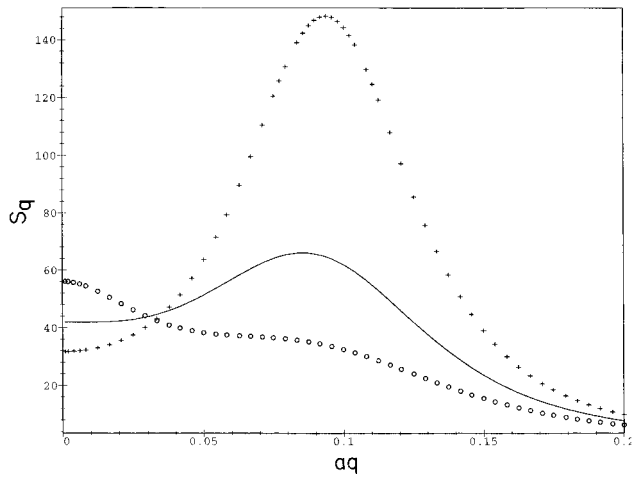

Figure 11. Effect of uniaxial extension ($\lambda_{||} = 2$) on gels studied at $\phi = \phi_{prep} = 0.05$ in a poor solvent ($|w|a^{-3} = 0.35$) in the absence of salt. The parameters are $R_c = 0.005$, $f^{(0)} = 0$, and $f = 0.018$. The structure factors for wave vectors along ($S_{q||}$) and normal ($S_{q\perp}$) to the stretching axis are shown by circles and crosses, respectively. The structure factor of an unstretched gel is shown for comparison (solid line).

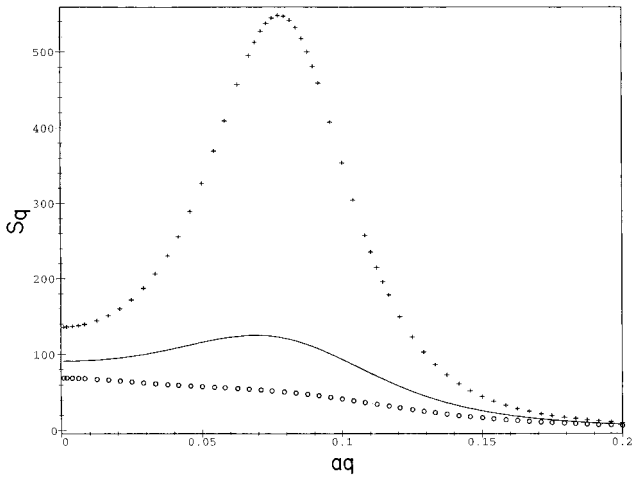

Figure 12. Effect of uniaxial extension on gels in the presence of added salt ($\hat{c}_s = 0.003$). All other parameters are the same as in Figure 8.

As shown in Figure 12, the magnitude of the peak intensity increases dramatically by the addition of even minute quantities of salt ($\hat{c}_s = 0.003$), as the presence of salt reduces the stability of the gel against microphase separation and decreases the critical wave vector **q***. Another interesting effect of added salt which can be clearly observed in Figure 12 is that the scattering in the direction normal to the extension axis becomes larger than that from an unstretched gel, throughout the entire range of wave vectors (the opposite effect is observed for the scattering along the stretching axis).

Inspection of the expressions for the correlators, eqs 10 and 11, shows that the sign of the angular anisotropy at $q = 0$ depends on the sign of the corresponding effective interaction coefficient, $\hat{w}_{\mathbf{q}=0}$, in eq 14. The ratio $(S_{\mathbf{q}||}/S_{\mathbf{q}\perp})_{\mathbf{q}\to 0}$ is larger than unity for $\hat{w}_{\mathbf{q}=0} > 0$ (this case is realized in Figure 11) and is smaller than unity in the reverse case (Figure 12). The coefficient $\hat{w}_{\mathbf{q}=0}$ can be positive even under poor solvent conditions, due to the positive electrostatic contribution to the second virial coefficient (it is always negative in the presence of large concentrations of added salt since the electrostatic contribution vanishes in this limit).

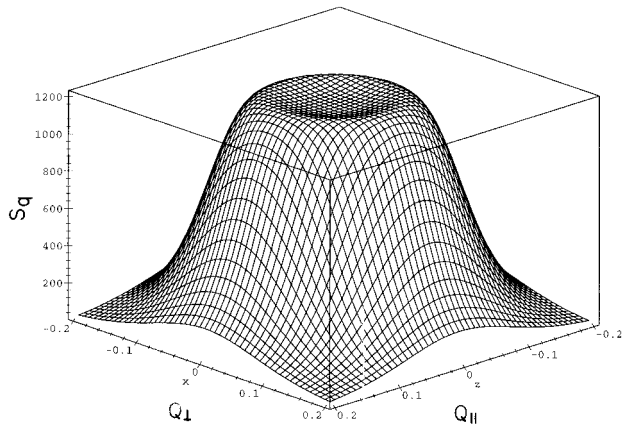

Figure 13. Three-dimensional plot of the structure factor in the ($Q_{||}$,$Q_\perp$) plane for an undeformed gel ($\lambda = 1$) studied at $\phi = 0.15$ in a poor solvent ($|w|a^{-3} = 0.51$) in the absence of salt. The parameters are $\phi_{prep} = 0.05$, $R_c = 0.01$, $f^{(0)} = 0$, and $f = 0.05$.

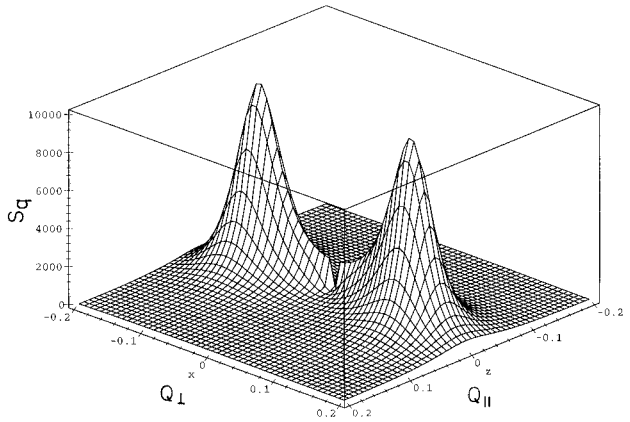

Figure 14. Three-dimensional plot of the structure factor in the ($Q_{||}$,$Q_\perp$) plane, for a uniaxially stretched gel ($\lambda = 1.4$). All other parameters are the same as in Figure 13.

In Figures 13 and 14 we present three-dimensional plots of the scattering profiles of a gel with concentration larger than ϕ_{prep}, studied close to the MSP. As expected, the maximum at q^* is isotropic (i.e., does not depend on the direction of **q***) in the absence of deformation. The angular degeneracy is removed by deformation and two distinct peaks oriented along the principal axes of compression are clearly observed in Figure 14. Comparison of Figures 13 and 14 shows that the overall intensity increases dramatically as the MSP line is pushed down by uniaxial extension.

The preceding discussion suggests an interesting possibility for studies of gels in electric fields. The modulation of the monomer density profile as the MSP is approached is accompanied by a corresponding modulation of the charge distribution. Below the MSP, the random orientation of the density gradients will produce no spontaneous dipole moment density, and the electric field will interact only with the induced dipole moment. At the MSP, the gel transforms into an aggregate of connected domains, each of which is characterized by a local spontaneous dipole moment. In both cases, the presence of an external electric field will result in the appearance of orientational ordering of the dipoles but the effect will be much larger at the MSP because of the ease with which the domains can be oriented by the field. This effect (as well as the effect of uniaxial stretching) can be observed by measuring the anisotropy

of polarized light scattering from charged gels in poor solvents.

4. Discussion

In this work we analyzed some of the rich physics of charged polymer gels. The new and unexpected results obtained in this work concern the existence of finite wavelength instabilities in the gel, associated with the onset of microphase separation. What distinguishes between microphase separation in gels and in other (complex fluid) systems is the fact that while in the latter the appearance of a peak in the scattering profile reflects the *enhancement of thermal fluctuations about the homogeneous equilibrium state of a liquid*, in gels the phenomenon is associated with the *reorganization of the local structure of an inhomogeneous solid* and the appearance of a spatial modulation in the equilibrium density profile at a wavelength $2\pi/q^*$, even before the onset of the microphase separation transition. Although the analysis of the modulated mesophases which appear at the MSP is beyond the scope of this work, it is plausible that the transition leads to the formation of lamellar domains, each of which is characterized by a different orientation of the lamellar planes. We predict that under uniaxial deformation, the "directors" of the domains become oriented along the principal axes of compression. Since periodic static density variations lead to the formation of permanent dipole moments, similar effects can be obtained by the application of electric fields.

Microphase separation is expected to have a dramatic effect on the mechanical properties of gels. At finite time scales, the resulting bicontinuous network of dense connected aggregates surrounded by solvent-rich domains should behave as a network with an increased effective degree of cross-linking and, consequently, the high-frequency modulus is expected to be larger than the static modulus of the homogeneous gel. An order of magnitude increase of the dynamic compressional modulus at the MSP was observed in recent mechanical experiments.[27]

The existence of the MSP has important ramifications for scattering experiments. Away from the LP, the peak in the scattered intensity is predicted to occur at wave vectors larger than the inverse monomer fluctuation radius (which is of the order of the mesh size) and can only be observed by neutron or X-ray scattering. The position of the peak varies with the thermodynamic parameters and passes through the visible range as the LP is approached, suggesting that this point can be detected by light scattering. With addition of salt, the line at which the structure factor diverges moves downward on the phase diagram, toward smaller values of $|w|$ (i.e., the MSP moves to smaller values of the Flory χ parameter). An interesting corollary of our results is the possibility of reentrant opalescence, i.e., that as one moves across the Lifshitz point (for example, by increasing the concentration), light scattering will first increase and then decrease again as the peak of the scattered intensity moves to $\mathbf{q}^* = 0$ (i.e., out of the visible range), and the gel will recover its "clear" appearance.

Similarly to the case of neutral gels, we find that the thermodynamic conditions in the state of preparation play an important role in determining the subsequent history of charged gels. The new feature characteristic of polyelectrolyte gels is that the memory of the electrostatic conditions at the state of preparation cannot be wiped out by the addition of salt in the final observed state of the network and that gels prepared by cross-linking from polyelectrolyte solutions will be more homogeneous than those prepared from solutions of neutral polymers.

Our detailed analysis of the scattering profiles shows a great variety of possible behaviors, which depend sensitively on the values of the thermodynamic parameters. In many cases we find that the scattered intensity changes non-monotonically with the wavelength. This suggests that neutron scattering experiments which probe the high q range give only partial information about the profile and that, in order to obtain a complete physical picture, they must be supplemented by light scattering experiments which probe the small q range.

The anisotropy of scattering from uniaxially stretched gels in Θ solvents is strongly wavelength dependent. In the vicinity of the peak in the structure factor, the scattering is enhanced in the plane normal to the stretching axis and is suppressed along this axis. The situation is reversed at $\mathbf{q} \to 0$ and we conclude that the usual butterfly effect should always be observed at sufficiently long wavelengths (i.e., in the light scattering range). However, since the angular anisotropy decreases with increasing degree of ionization, it may fall below experimental resolution for strongly charged gels in the absence of salt (butterfly patterns will reappear when salt is added to the system).

The situation is even more complicated for charged gels in poor solvents. Under uniaxial extension, the angular anisotropy in the vicinity of the peak in the structure factor behaves in a way which is qualitatively similar to the Θ solvent case. However, in the $\mathbf{q} \to 0$ limit, the sign of the anisotropy ($S_{q\parallel} - S_{q\perp}$) is determined by the sign of the effective interaction coefficient $\hat{w}_{\mathbf{q}\to 0}$ and changes from positive to negative with the addition of salt or with decreasing solvent quality. In the vicinity of the Lifshitz point the structure factor exhibits a single maximum at $\mathbf{q} = 0$ and under uniaxial extension both normal and inverted (i.e., rotated by 90°) butterfly patterns can be observed, depending on the location on the phase diagram, since the sign of $\hat{w}_{\mathbf{q}\to 0}$ changes from positive to negative as the spinodal is approached.

Although this work deals with charged gels, the scattering profiles of neutral gels in poor solvents (held at a fixed volume) can be obtained by setting $f^{(0)} = f = 0$ in the corresponding expressions. In this case, phase separation takes place when $w < 0$ ($\chi > {}^1/_2$) and both SP and MSP scenarios are possible, depending on the concentration. For gels prepared in a good solvent the Lifshitz point, which defines the crossover between the SP and the MSP regimes, can be reached by studying the gel at $\phi = \phi_{\text{prep}}^{5/8}$, and for gels prepared in Θ solvents the corresponding concentration is $\phi = \phi_{\text{prep}}$. Away from the LP the critical wave vector at the MSP is of the order of the inverse monomer fluctuation radius, $q^* \simeq 1/(a\bar{N}^{1/2})$.

Our results lead to the following simple physical picture of the effect of uniaxial deformation on neutral and charged gels (see Figure 15). Away from the phase separation spinodal, uniaxial extension results in the appearance of a long-wavelength, finite-amplitude modulation of the static density profile, directed parallel to the extension (or normal to the compression) axis. When the spinodal line is approached, the picture is reversed: the static density profile becomes modulated normal to the stretching (or parallel to the compression) direction, with an amplitude which diverges at the spinodal. The critical wave vector of the modulation

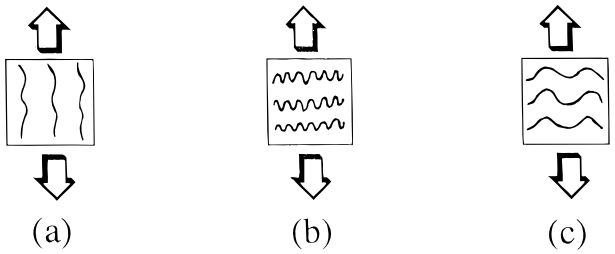

Figure 15. Schematic drawing of the monomer density profile of uniaxially stretched gels: (a) away from the instability line; (b) near the MSP; (c) near the SP. The elongation axis is indicated by arrows.

q^* is finite near the MSP and vanishes near the SP. The transition between the two regimes takes place at the LP.

The most direct indication of the existence of the microphase separation transition comes from neutron scattering experiments on NIPA/AAc gels studied near their volume transition temperature,[17] in which a dramatic increase of the scattered intensity at a finite $q = q^*$ was observed. It was assumed that the scattering is dominated by thermal fluctuations and the results were analyzed in the spirit of the theory[11] of polyelectrolyte solutions. We predict that the observed enhancement is dominated by the scattering from static inhomogeneities which diverges as $[w - w_{MSP} + c(\mathbf{q}^2 - \mathbf{q}^{*2})^2]^{-2}$ as the MSP is approached (the thermal scattering diverges as $[w - w_{MSP} + c(\mathbf{q}^2 - \mathbf{q}^{*2})^2]^{-1}$). This agrees with the observed $\mathbf{q}^{-4}$ dependence of the scattered intensity in the high-q limit. The observation that the concentration dependence of the critical wave vector q^* deviates from the Borue−Erukhimovich prediction is in accord with our results. New scattering experiments which systematically probe the entire range of wavelengths and thermodynamic parameters covered by the theory are clearly necessary in order to promote our understanding of the physics of phase separation in charged gels.

Finally, we would like to discuss the various assumptions and approximations used in our work, some of which are common to neutral and charged gels and have been discussed in detail elsewhere.[4,5] These include the usual assumptions of the Edwards model of randomly cross-linked gels[28] such as the neglect of topological entanglements as well as the assumption of small amplitude of static density inhomogeneities (the latter is valid for networks prepared away from the "cross-link saturation threshold"[4,5]). In order to reduce the number of free parameters, we considered only gels prepared in a good solvent in the absence of added salt. The study of gels prepared in poor solvents is beyond the scope of the present approach, since this would result in an extremely inhomogeneous distribution of cross-links and our random phase approximation for the static density inhomogeneities[4,5] would break down.

In order to describe the electrostatics of charged gels, we considered the case of small fluctuations of the charge density and derived the Debye−Hückel structure factor. Furthermore, we considered only sufficiently small degrees of ionization, for which the effect of charges on the conformations of the polymer chains is negligible. Unfortunately, most of the experiments to date were performed at degrees of ionization[7] which fall outside the domain of applicability of our model. Nevertheless, since in this range the counterion entropy dominates over electrostatic corrections to the elastic free energy (due to the effect of charges on the conformation of the chains), our theory is expected to provide a reasonable qualitative description of the experimental results. Indeed, to the best of our knowledge, all available experimental data on charged gels in poor solvents are consistent with our predictions.

All the above approximations can have a quantitative effect on our results but are not expected to change their qualitative behavior. The major assumption which may affect the validity of our results is that the spinodal instability begins from a microscopically homogeneous state of the gel, before macrophase separation has taken place by nucleation of the new phase. Although nucleation in the bulk is strongly suppressed by the distortion of the elastic field in three-dimensional gels,[29] macrophase separation can occur on the gel surface and is expected to lead to the formation of a stable surface layer of the new phase.[23,30,31] Bulk nucleation is possible in one dimension and may result in coexisting bulk phases in thin rodlike gels.[32] The resulting phases are, in general, macroscopically inhomogeneous and anisotropic and their spinodal instabilities cannot be described by the present approach.

Acknowledgment. This research was supported by grants from the Israeli Academy of Sciences and Humanities, the Israeli Ministry of Science and Technology, and the Bar-Ilan University. S.P. acknowledges financial support from the Soros Foundation.

References and Notes

(1) Annaka, M.; Tanaka, T. *Nature* **1992**, *355*, 430.
(2) de Gennes, P.-G. *Scaling Concepts in Polymer Physics*; Cornell University Press: Ithaca, NY, 1979.
(3) des Cloizeaux, J.; Jannink, G. *Polymers in Solution. Their Modelling and Structure*; Clarendon Press: Oxford, 1990.
(4) Panyukov, S.; Rabin, Y. *Phys. Rep.* **1996**, *269*, 1.
(5) Panyukov, S.; Rabin, Y. *Macromolecules* **1996**, *29*, 7900.
(6) Rabin, Y.; Panyukov, S. *J. Comput.-Aided Mater. Des.* **1996**, *3*, 281.
(7) Bastide, J.; Candau, S. J. In *Physical Properties of Gels*; Cohen-Addad, J. P., Ed.; Wiley: Chichester, 1996.
(8) Schosseler, F.; Illmain, F.; Candau, S. J. *Macromolecules* **1991**, *24*, 225.
(9) Mendes, E.; et al. *Europhys. Lett.* **1995**, *32*, 273.
(10) Moussaid, A.; et al. *J. Phys. II* **1993**, *3*, 573.
(11) Borue, V.; Erukhimovich, I. *Macromolecules* **1988**, *21*, 3240.
(12) Joanny, J. F.; Leibler, L. *J. Phys. (Paris)* **1990**, *51*, 545.
(13) Schosseler, F.; et al. *J. Phys. II* **1994**, *4*, 1221.
(14) Horenreich, R.; Luban, M.; Shtrikman, S. *Phys. Rev. Lett.* **1982**, *35*, 1678.
(15) Leibler, L. *Macromolecules* **1980**, *13*, 1602.
(16) de Gennes, P. G. *The Physics of Liquid Crystals*; Clarendon: Oxford, 1974.
(17) Shibayama, M.; Tanaka, T.; Han, C. C. *J. Chem. Phys.* **1992**, *97*, 6842.
(18) Marko, J.; Rabin, Y. *Macromolecules* **1992**, *25*, 1503.
(19) Odijk, T. *J. Polym. Sci., Polym. Phys. Ed.* **1977**, *15*, 477.
(20) Shibayama, M.; Tanaka, T.; Han, C. C. *J. Chem. Phys.* **1992**, *97*, 6829.
(21) Panyukov, S. *JETP Lett.* **1990**, *51*, 253. Panyukov, S. *Sov. Phys.—JETP* **1990**, *71*, 372.
(22) Onuki, A. *Adv. Polym. Sci.* **1993**, *109*, 63.
(23) Panyukov, S.; Rabin, Y. *Macromolecules*, in press.
(24) Rabin, Y.; Onuki, A. *Macromolecules* **1994**, *27*, 870.
(25) Tokita, M.; Tanaka, T. *Science* **1991**, *253*, 1121.
(26) Bekiranov, S.; Bruinsma, R.; Pincus, P. *Europhys. Lett.* **1993**, *24*, 183.
(27) Shibayama, M.; Morimoto, M.; Nomura, S. *Macromolecules* **1994**, *27*, 5060.
(28) Deam, R. T.; Edwards, S. F. *Philos. Trans. R. Soc. London, Ser. A* **1976**, *280*, 317.
(29) Onuki, A. *Phys. Rev. A* **1988**, *38*, 2192.
(30) Matsuo, E. S.; Tanaka, T. *J. Chem. Phys.* **1988**, *89*, 1695.
(31) Sekimoto, K. *Phys. Rev. Lett.* **1993**, *70*, 4154.
(32) Hirotsu, S. *J. Chem. Phys.* **1988**, *88*, 427.

MA960826E